Science Advances
AAAS

advances.sciencemag.org/cgi/content/full/4/6/eaat0911/DC1

Supplementary Materials for

Direct metabolite detection with an n-type accumulation mode organic electrochemical transistor

Anna Maria Pappa, David Ohayon, Alexander Giovannitti, Iuliana Petruta Maria, Achilleas Savva, Ilke Uguz, Jonathan Rivnay, Iain McCulloch, Róisín M. Owens, Sahika Inal

Published 22 June 2018, *Sci. Adv.* **4**, eaat0911 (2018)
DOI: 10.1126/sciadv.aat0911

This PDF file includes:

- fig. S1. The output and transfer characteristics of a typical all n-type polymer (P-90)–based OECT.
- fig. S2. Transfer curves of the OECT in the absence and presence of the enzymatic reaction.
- fig. S3. Calibration curve relating the NR of the device to a range of lactate concentrations.
- fig. S4. QCM-D response of the P-90–coated sensor immersed in PBS.
- fig. S5. AFM topography images of the P-90 film coated on Au substrate.
- fig. S6. The CV curve of the P-90 film before and after addition of the enzyme into the PBS solution and a scheme of bioelectrocatalytic reactions.
- fig. S7. The effect of pH on the CV curve of the P-90 film.
- fig. S8. The changes in the absorbance spectrum of the P-90 film during the electrochemical switch.
- fig. S9. The effect of air on the reaction of lactate with LOx-functionalized P-90.
- fig. S10. Sensitivity of the device to lactate and when operated under different biasing conditions at the channel and the gate.

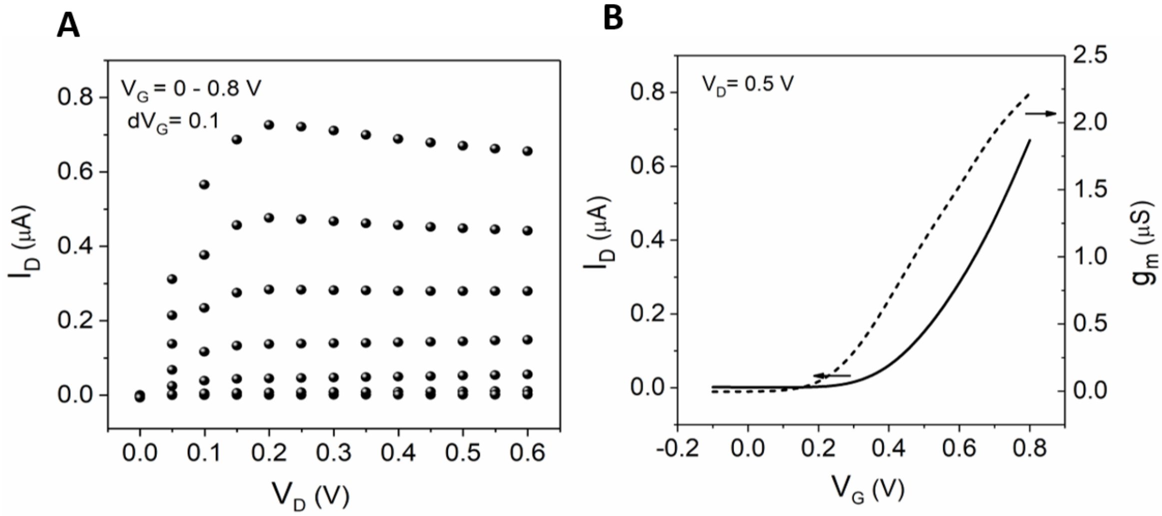

fig. S1. The output and transfer characteristics of a typical all n-type polymer (P-90)–based OECT. The corresponding transconductance values (g_m) are shown in (**B**) along with the transfer curve (V_D=0.5 V). The channel has a thickness, width and length of ca. 100 nm, 100 µm and 10 µm, respectively. The electrolyte is PBS.

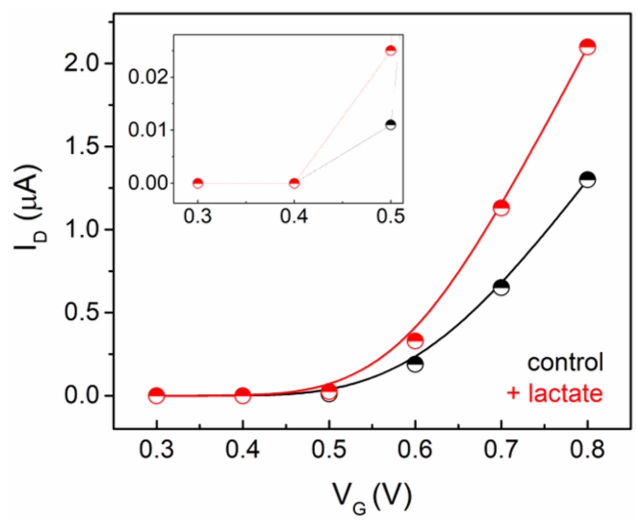

fig. S2. Transfer curves of the OECT in the absence and presence of the enzymatic reaction. The curves show the increase in I_D as a function of V_G (V_D=0.5V) in the presence (red line) and absence (black line) of lactate in the solution containing LOx. The onset V_G that needs to be applied for sensing lactate corresponds to the actual onset voltage of the device. The inset shows the magnified response of the device at low V_G.

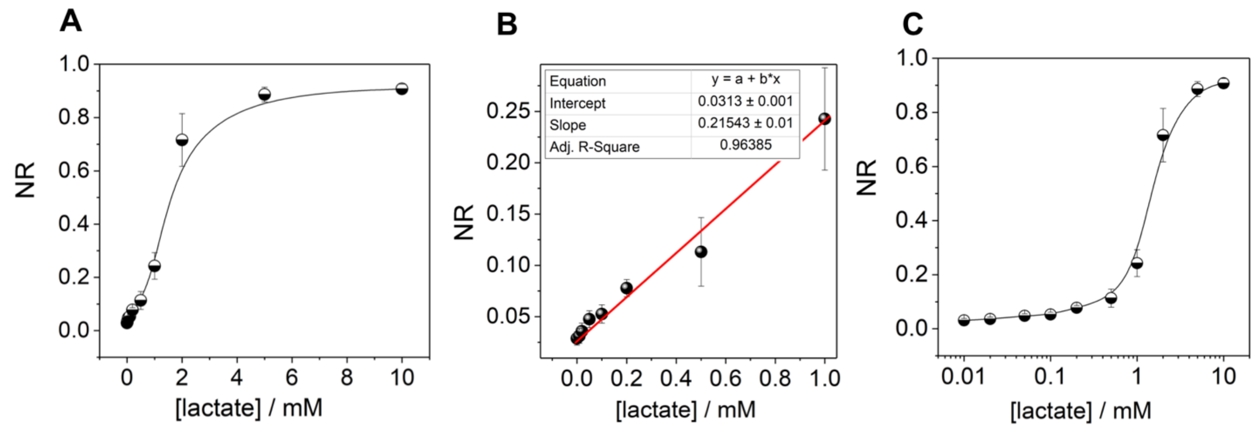

fig. S3. Calibration curve relating the NR of the device to a range of lactate concentrations. (**A**) in linear scale, (**B**) magnifying the linear part of the curve (from 10 μM to 1 mM), and finally (**C**) in logarithmic scale. Error bars represent the standard deviation from the mean value (n=4). In B, the linear interpolation of the calibration curve, with an adjusted R-squared value of ~0.96, indicates a linear regression up to 1 mM of lactate. The slope, calculated to be ~0.214 expresses the sensitivity of the device per mM of lactate concentration. $NR = |\frac{I}{I_{max}}|$, where I and $I_{\max}$ are the current output at a given lactate concentration and the maximum current output of the device at the maximum applied gate potential in the absence of lactate, respectively).

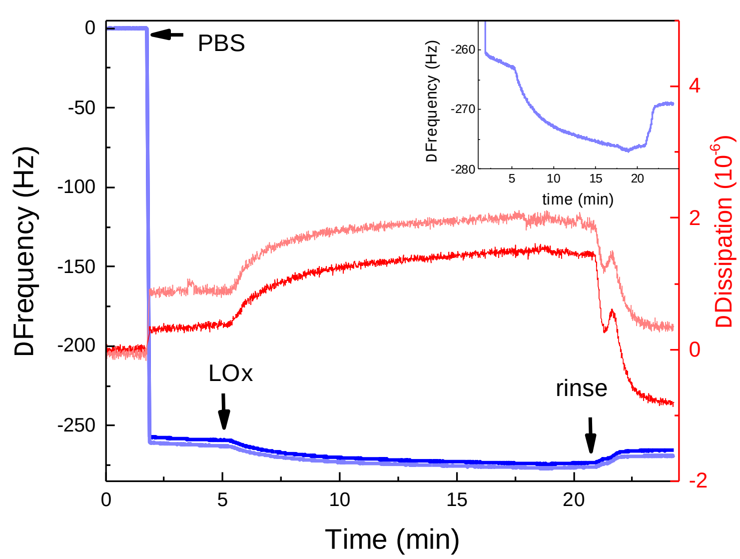

fig. S4. QCM-D response of the P-90–coated sensor immersed in PBS. Left axis shows the change in frequency and the right one of the dissipation for the overtones 5[th] and 7[th]. The film is first in air, then exposed to PBS which is followed by the introduction of LOx in PBS and is finally rinsed with PBS. The mass change is calculated treating this data with viscoelastic model. The inset is a magnification of the change in frequency (5[th] overtone) as the enzyme is injected into the PBS solution flowing over the film.

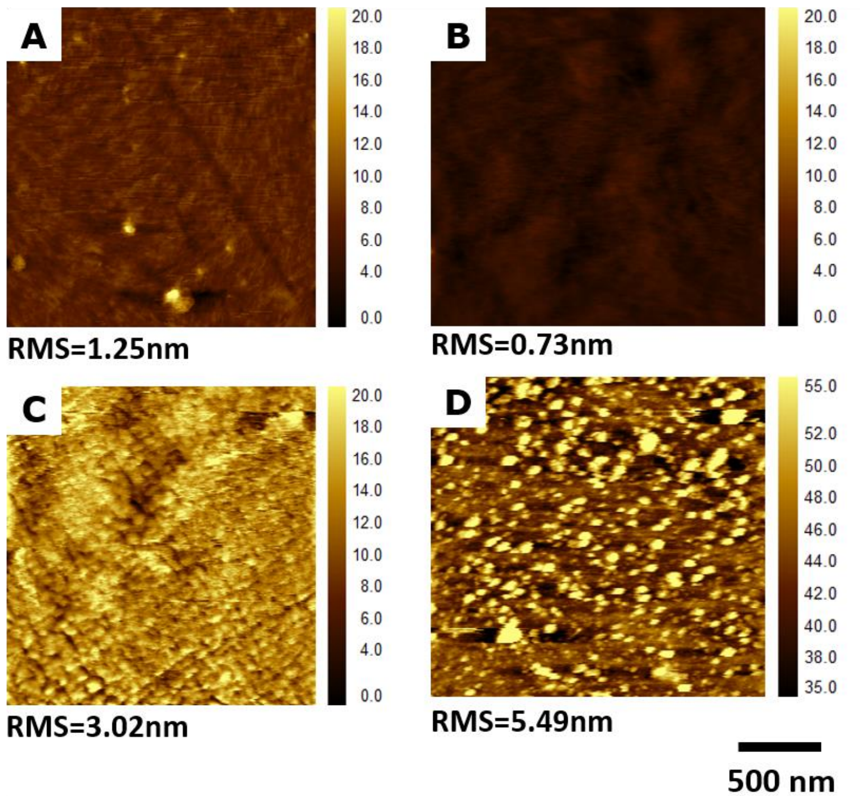

fig. S5. AFM topography images of the P-90 film coated on Au substrate. (**A**) in air, (**B**) immersed in PBS and (**C**) exposed to LOx, as well as (**D**) rinsed with PBS solution upon the incubation with the enzyme.

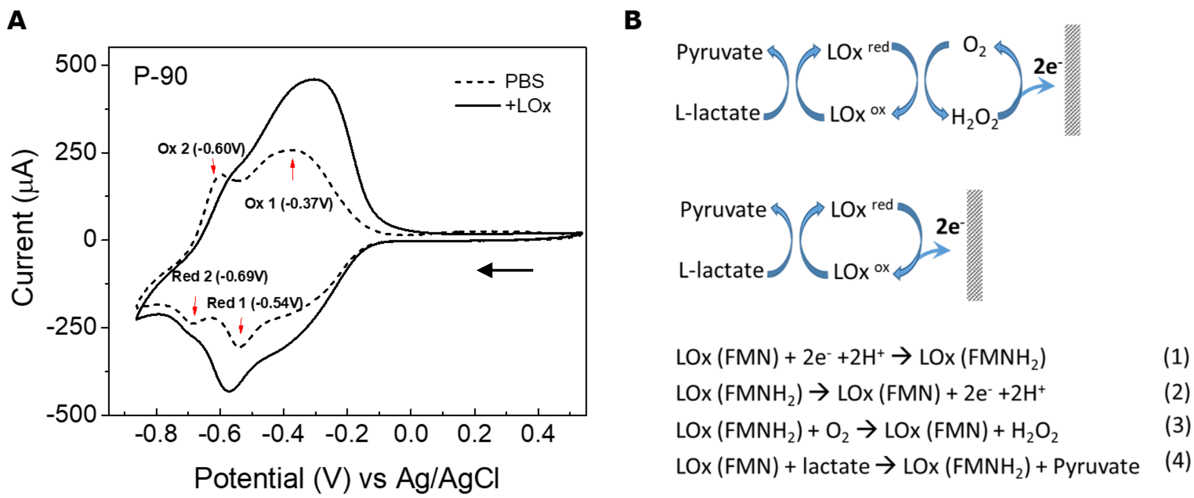

fig. S6. The CV curve of the P-90 film before and after addition of the enzyme into the PBS solution and a scheme of bioelectrocatalytic reactions. (**A**) CV curve shows the peak positions of the two prominent redox couples (Red/Ox 1 and Red/Ox 2) of the material (dashed lines). Enzyme addition causes a change in the shape of the curve (solid lines). Scan rate is 50 mVs^{-1} and the scanning bias is in the backward direction. (**B**) The reaction cycles in the presence and absence of O_2, with the associated redox reactions.

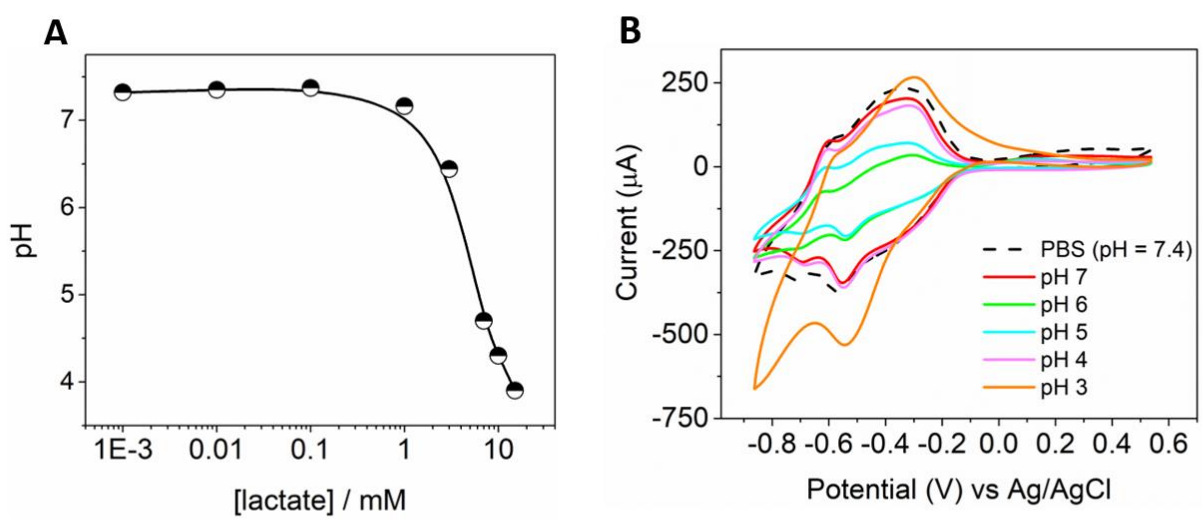

fig. S7. The effect of pH on the CV curve of the P-90 film. (**A**) The change in pH of the solution containing LOx as a function of lactate concentration, (**B**) the CV curves of P-90 film recorded in solutions of different pH.

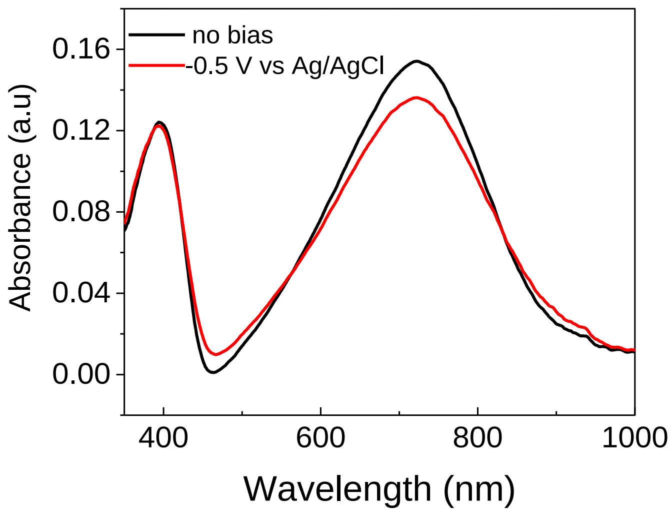

fig. S8. The changes in the absorbance spectrum of the P-90 film during the electrochemical switch. The absorbance spectrum of the film coated on an ITO substrate measured in PBS with and without applied bias (-0.5V *vs* Ag/AgCl).

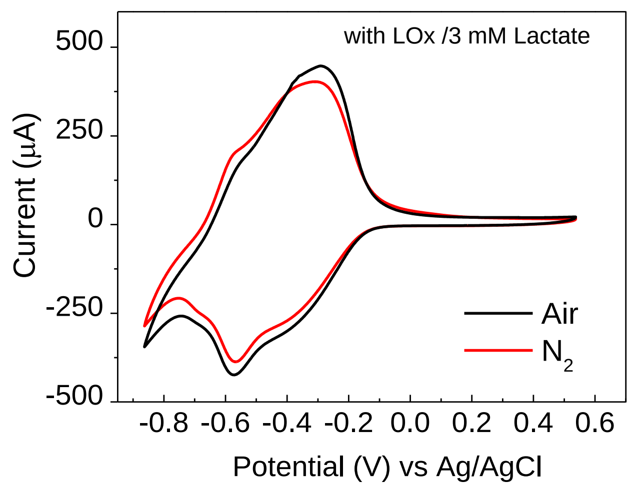

fig. S9. The effect of air on the reaction of lactate with LOx-functionalized P-90. CV curve of the P-90 film in air (black) and N_2 (red) saturated PBS solution. The solution includes LOx and 3 mM of lactate.

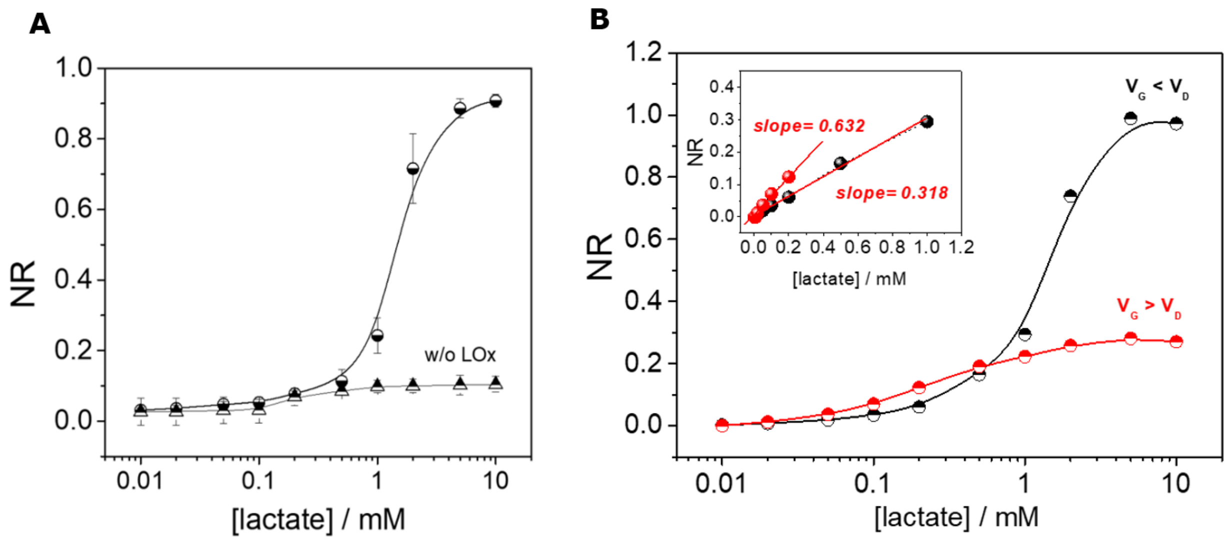

fig. S10. Sensitivity of the device to lactate and when operated under different biasing conditions at the channel and the gate. (**A**) The device response to lactate in the presence (circles) and in the absence (triangles) of the enzyme, LOx. (**B**) The device is operated at a V_G of 0.5 V and V_D of 0.7 V (black), or at V_G = 0.7 V and V_D = 0.5 V (red). The inset shows the response of the device to lactate, represented in linear scale, with the slope quantifying the sensitivity.